Experimental observation of 1/f noise in quasi-bidimensionnal turbulent flows

J. HERAULT[1], F. PÉTRÉLIS[1] and S. FAUVE[1]

[1] *Laboratoire de Physique Statistique, Ecole Normale Supérieure, CNRS, Université P. et M. Curie, Université Paris Diderot, Paris, France*

arXiv:1605.09664v1 [physics.flu-dyn] 31 May 2016

PACS 47.27.-i – Turbulent flows
PACS 47.27De – Coherent structures
PACS 05.40.-a – Fluctuation phenomena, random processes, noise, and Brownian motion

Abstract. - We report the experimental observation of $1/f^{\alpha}$ noise in quasi-bidimensionnal turbulence of an electromagnetically forced flow. The large scale velocity U_L exhibits this power-law spectrum with $\alpha \simeq 0.7$ over a range of frequencies smaller than both the characteristic turn-over frequency and the damping rate of the flow. By studying the statistical properties of sojourn time in each polarity of U_L, we demonstrate that the $1/f^{\alpha}$ noise is generated by a renewal process, defined by a two-state model given by the polarities of the large scale circulation. The statistical properties of this renewal process are shown to control the value of the exponent α.

Introduction. – Fluctuations which have spectral densities varying approximately as $1/f$ (or more generally as $1/f^{\alpha}$ with $0 < \alpha < 2$) over a large range of frequencies, or $1/f$ noise, have been studied since a long time in physics, first in the context of low frequency voltage fluctuations in electrical conductors [1]. An early motivation has been the divergence problem related to a spectrum with a $1/f$ power law without any observed low frequency cut-off. Other questions concerned the non stationary or non Gaussian character of $1/f$ noise. The $1/f$ behavior has been first related to the existence of a broad band distribution of relaxation times in the system [2, 3]. Other stochastic models include fractal Brownian motion [4] or power-law shot noise [5]. Dynamical system theory provided another type of approach relying on deterministic low dimensional systems displaying a transition to chaos via intermittency [6, 7]. These studies were useful to explain both the wide (power-law) distribution of relaxation times as well as the related $1/f^{\alpha}$ spectrum. This correspondence has been emphasized using purely stochastic models that involve random bursts or random switching between two states. It has been shown that if the intereventtime probability distribution function (PDF) decays as a power law, $P(\tau) \propto \tau^{-\beta}$, a $1/f^{\alpha}$ spectrum is obtained with α related to β [8, 9]. Most of the early experimental observations of $1/f^{\alpha}$ noise do not display such discrete events. However, switching events have been observed in small electronic systems (submicrometer MOSFETs) [10] and more recently in blinking quantum dots [11].

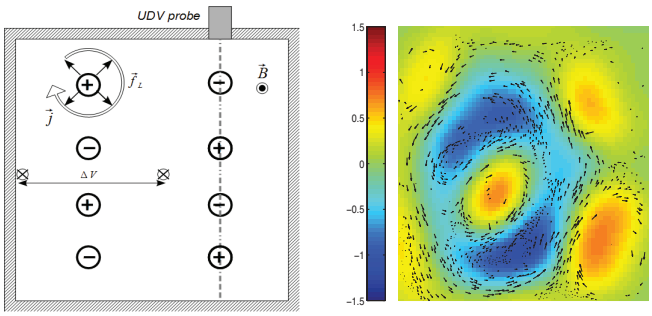

Fig. 1: (Color online) Left : experimental set-up. The current injected through the electrodes and the vertically applied magnetic field induce an azimuthal Lorentz force close to each electrode. A pair of probes measure a potential difference ΔV, proportional to the flow rate between the probes. The velocity component along the dashed line is measured using ultrasonic Doppler velocimetry. Right: Particle tracking of oxide tracers are used to compute the large scale vorticity levels in s^{-1}. Arrows represent the velocity field (Rh=23.5).

We present here the observation of a similar behavior on a macroscopic system, two-dimensional (2D) turbulence, where we show that switching events between the two polarities of the large scale circulation (LSC) account for the observed $1/f^{\alpha}$ noise. $1/f^{\alpha}$ spectra have been reported in various turbulent flows: in wall turbulence, they are observed in an intermediate

frequency range and are ascribed to the $1/k$ spatial spectrum related to hairpin vortices [12]. They have been observed for all frequencies below the integral scale in von Karman swirling flows, both for the pressure [13] and the velocity [14]. $1/f^{\alpha}$ spectra have been also observed in these flows for the fluctuations of the magnetic field, either when an external field is applied to a liquid metal [15] or when the magnetic field is generated through the dynamo process [16]. Similar results have been found in numerical simulations of hydrodynamic or magnetohydrodynamic turbulence [17].

The experiment under study consists in a quasi-bidimensional flow of a thin layer of liquid metal driven by a spatially periodic electromagnetic force. It has been predicted [18] and experimentally checked [19, 20] that in 2D turbulence, an inverse cascade of energy can drive a LSC superimposed on turbulent fluctuations. Whereas many studies have focused on the relation between coherent structures and spatial spectra, less attention has been paid to the frequency spectrum of 2D turbulent flows and to the possible signature of the dynamics of coherent structures. We study the temporal and spectral properties of the LSC and report the first experimental study of $1/f^{\alpha}$ noise in 2D turbulence. A striking feature of these fluctuations is their frequency range, which is well below the LSC turnover frequency and damping rate and extends to the lowest measured frequency without any low frequency cut-off. We explain how this $1/f^{\alpha}$ spectrum results from the dynamics of the LSC and we show that α is related to the power-law exponent β of the PDF of the waiting time between two successive changes of sign of the LSC.

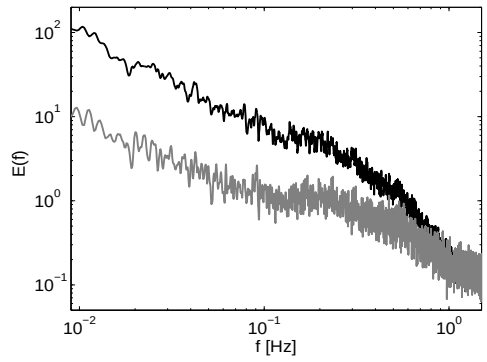

Fig. 2: Frequency power spectra $E(f)$ of one component of the velocity field for $Rh = 26$: local velocity (grey), velocity averaged on the length of the cell (black).

Experimental set-up and techniques. – A thin layer of liquid metal (Galinstan) of thickness $h = 2\,\mathrm{cm}$, is contained in a square cell of length $L = 12cm$ submitted to a uniform vertical magnetic field up to $B_0 \simeq 0.1$T. A DC current I (0-200A) is injected at the bottom of the cell through an array of 8 electrodes of diameter $d = 8\,\mathrm{mm}$ flush to the bottom of the fluid layer (see Fig.1). In the vicinity of each electrode, the current density $\mathbf{j}$ is radial so that the associated Lorentz force $\mathbf{f}_L = \mathbf{j} \times \mathbf{B}_0$ creates a local torque. For low injected current, this forcing drives a laminar flow made of an array of 8 counter-rotating vortices. Great care has been paid to inject the same current through each electrode, in order to avoid the injection of net angular momentum in the flow. To prevent the oxidation of the upper surface, a thin layer of hydrochloric acid is placed on top of the liquid metal. Balancing the Lorentz force and the inertia gives the typical velocity of the forced vortices, $U_c = \sqrt{|\mathbf{f}_L|L}$. Its order of magnitude is $10^{-1}m/s$ for $25 < I < 100$ A. The bidimensionality of the flow is achieved by a low magnetic Reynolds number, typically $Rm = \sigma\mu U_c L \sim 10^{-2}$, a relatively high interaction parameter $N = \sigma B_0^2 L/(\rho U_c) \sim 10$ and a high Hartmann Number $\mathrm{Ha} = hB_0[\sigma/(\rho\nu)]^{1/2} \sim 10^2$, where μ_0, σ , ν are the magnetic permeability, electrical conductivity and kinematic viscosity respectively. In this parameter range, the velocity does not depend on the vertical coordinate except in a thin Hartman layer of size $\delta_h = h/\mathrm{Ha}$ along the bottom boundary. This provides an additional dissipation to the 2D depth-averaged velocity field $\mathbf{v}(x,y,t)$ that takes the form of a linear friction term in the 2D Navier-Stokes equation, namely $-\mathbf{v}/\tau_H$ [21], with a time scale $\tau_H = h\delta_H/\nu$ of the order of $10\,s$. We have checked that τ_H is in good agreement with the experimentally measured damping rate of the large scale flow [22], confirming the bidimensionality of the flow as explained in [21, 23].

For the 2D flow, we define two non-dimensional parameters from the two sources of dissipation, viscosity and friction: the usual Reynolds number $Re = U_c L/\nu$ and $Rh = U_c\tau_H/L$ which is the ratio of inertia to linear friction. The ratio Re/Rh, independent of the injected current, is equal to $\mathrm{Ha}(L/h)^2 \sim 10^4$. By changing I we vary Rh between 1 and 50 so that we reach relatively large Reynolds numbers. Since viscous dissipation becomes efficient at scales smaller than $l = L\sqrt{Rh/Re} \sim 10^{-3}m$, dissipation at large scale is mainly due to friction. It follows from these order of magnitude estimates that Rh is the pertinent control parameter for the dynamics of the large scales, which is well verified experimentally [22].

Velocity measurements are performed using three different methods [22]: particle tracking (oxides on the Galinstan surface) shows the large scale velocity and the corresponding vorticity levels as displayed in Fig.1. An ultrasound transducer emits 4 MHz wave trains along the dashed line in Fig. 1. They are reflected back by oxide particles in the flow and analyzed using a DOP3010 velocimeter (Signal Processing). The longitudinal velocity component is thus measured throughout the cell. The power spectra of the local velocity in the bulk of the cell and of the averaged velocity along the dashed line in Fig. 1, are shown in Fig. 2. They both display a power law behavior close to $1/f$ on a decade $0.01 < f < 0.1$ Hz. However, this measurement method is not well suited in the low frequency limit because measurements of long duration (> 5 hours) are difficult due to the large memory required to save and to process the data. It has been known since a long time that a large scale velocity component can be directly determined by measurement the potential difference between a pair of electrodes in an external magnetic field [24]. As sketched in Fig. 1, one of the electrodes is located in the middle of the cell and the other one close to the lateral wall, 5 mm away from it. The potential

difference between the electrodes ΔV is $\Delta V \simeq \phi_L B_0$, with ϕ_L the flow rate between the center and the wall of the cell. In the following we use the spatially averaged velocity U_L, defined by $U_L = 2\phi_L/L$, which is thus the large scale velocity coarse-grained on size $L/2$.

The different flow regimes and the low frequency spectrum. – Increasing Rh from small values, coherent structures, with scales larger than the one of the forcing, are generated due to the non-linear energy transfers from small to large scales. For $Rh > 5$, the flow is turbulent and several spatial scales contain energy as displayed in Fig 1 (right). The dynamics of the LSC is chaotic. Its probability density function (PDF) is gaussian for intermediate values of Rh but becomes bimodal for $Rh > 12$. The LSC then reverses between two values $\pm U_L$ of maximum probability. When Rh is larger ($Rh \sim 30-40$), reversals of the LSC are less frequent and more visible on the direct recording of the velocity. They are no longer observed for $Rh > 50$, for which the LSC has a constant sign. All these flow regimes have been observed by numerical simulation of the 2D Navier-Stokes equation with damping [25]. The amplitude of the LSC given by the time series of U_L, is displayed in Fig. 3 for $Rh = 17$. High frequency turbulent fluctuations are superimposed to low frequency fluctuations. In particular we observe long events of constant sign (see for instance $307 < t < 340$ s).

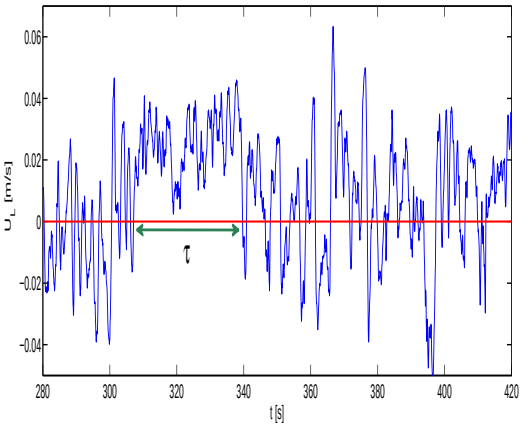

Fig. 3: Time series of $U_L(t)$ for $Rh = 17$. The velocity strongly fluctuates around zero, but events of constant polarity of duration $\tau > L/\langle|U_L|\rangle$ occur.

To investigate the properties of the LSC, we calculate the temporal power spectrum $E(f)$ of U_L (see Fig. 4). Two distinct behaviors are observed (for f larger or smaller than a crossover frequency f_t). The spectrum is steep for $f > f_t$. For $f < f_t$, the spectrum displays a power-law behavior $f^{-\alpha}$ with $\alpha = 0.7$. For $Rh < 30$, the large scale flow thus exhibits $1/f$ noise over roughly two decades. For $Rh > 30$, we observe a departure from the $f^{-0.7}$ scaling. This phenomenon is related to the transition of the flow to the condensed regime where the statistical properties of the flow suddenly change [18, 19]. For small values of Rh (between 5 and 10), the fluctuations of the LSC have a flat temporal power spectrum at small frequency. We thus restrict our study to $12 < Rh < 30$. We report the values of the exponent α (blue circles) as a function of Rh in Fig. 5. The exponent is calculated on the interval $[f_c, f_t]$ where $f_c/(2\pi)$ is the inverse of the experiment duration which is set by the thermal stability of the set-up, of the order of a few hours.

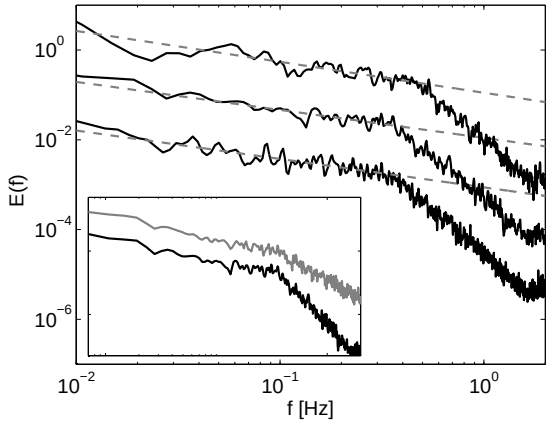

Fig. 4: Frequency power spectra $E(f)$ of $U_L(t)$ for $Rh = 16, 19, 24$, from the bottom to the top. Spectra have been shifted for clarity. The dashed lines are the best fits of the low frequency part of the spectra. Inset: frequency power spectra of U_L (black), of the sign of U_L (grey).

For frequencies larger than f_c, there is no sign of a frequency cut-off below which the spectrum would become flat. The maximum frequency f_t is of order 0.4 Hz and corresponds to several turnover times of the LSC $L/\langle|U_L|\rangle$, with $\langle|U_L|\rangle \sim 2.10^{-2} m/s$, a typical value of the time average of $|U_L|$. The low frequency range corresponds to frequencies smaller than the slowest turnover time. Obviously there is no hope that a Taylor hypothesis could explain the spectrum by an equivalence between frequency and wave number k. In addition, the $1/f$ range extends to frequencies much smaller than the damping rate $1/\tau_h = 0.1$ Hz. In other words, the $1/f$ spectrum is the frequency signature of large scale coherent structures, with life time larger than both their turnover time and the dissipation time τ_H.

Relation between the low frequency spectrum and reversals of the large scale velocity. – As noticed in Fig. 3, the LSC can maintain a constant direction for very long durations and a natural question is the relation between these events of constant polarity and the $1/f$ noise. To what extent do these events control the low frequency part of the spectrum? To answer this question, we compute E_S, the power spectrum of the sign of U_L, thus keeping only the information of the direction of rotation of the LSC. E_S is displayed in the inset of Fig. 4. It exhibits strong similarities with the spectrum of U_L for $f < f_t$. These observations are confirmed by the calculation of the exponent α_S (see Fig. 5), defined by $E_S(f) \propto f^{-\alpha_S}$ for $f < f_t$. For all Rh, α and α_S are almost equal, which implies that E_S and E contain the same spectral information for the low frequency range.

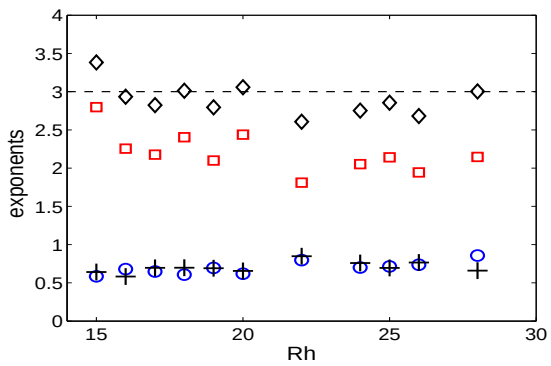

Fig. 5: (Color online) Exponents α ($\circ$) and α_S ($+$) of the power law of the spectra $E(f)$ and $E_S(f)$. Exponent β ($\square$) of the power law $P(\tau)$. $\alpha+\beta$ ($\diamond$) is nearly equal to 3.

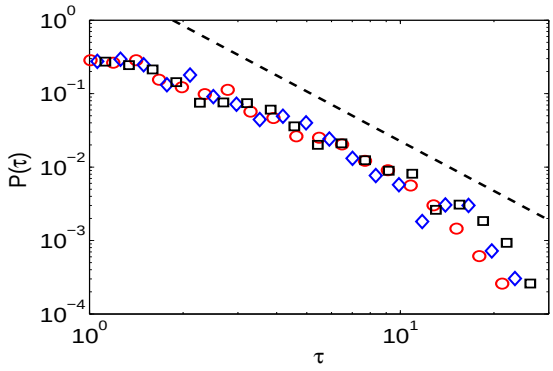

Fig. 6: (Color online) Probability density function $P(\tau)$ of duration τ between two consecutive sign changes for $Rh = 16\,(\circ), 19\,(\square), 24\,(\diamond)$. Dashed line: $\tau^{-\beta}$ with $\beta = 2.25$

To further investigate the information contained in the sign of U_L, we calculate the statistical properties of the time between sign changes. The PDF $P(\tau)$ of duration τ between two consecutive sign changes is shown in Fig. 6. $P(\tau)$ exhibits a power law, $P(\tau) \propto \tau^{-\beta}$ for $\tau > 4$ s, which corresponds to time scales larger than f_t^{-1}. The dashed line is a power law with $\beta = 2.25$. Such heavy-tailed distributions indicate that long durations have a high probability of occurrence. Then these events control the behavior of the autocorrelation function of the signal and thus are responsible for the form of the spectrum at low frequency. A simple argument can be stated as follows. Let $u(t)$ be the renewal process defined by the sign of U_L. We note T_i the interval between sign changes and consider the autocorrelation function $C(\tau) = \langle u(t)u(t+\tau)\rangle$. We estimate $C(\tau)$ as $T_m^{-1}\int_0^{T_m} u(t)u(t+\tau)dt$, with T_m tending to infinity. This corresponds to averaging the signal with itself but shifted in time, so that only phases for which the signal is constant on duration T_i larger than τ give a non zero contribution to $C(\tau)$. During T_m there are $T_m P(T_i)dT_i/\langle T_i\rangle$ phases of duration T_i which contribute $(T_i-\tau)$ to $C(\tau)$. We thus have $C(\tau) \propto \langle T_i\rangle^{-1}\int_0^{T_m} P(T_i)(T_i-\tau)dT_i$ which leads to $C(\tau) \propto \tau^{2-\beta}$. The associated spectrum follows from Wiener-Khinchin theorem, $E(f) \propto f^{\beta-3}$. We have thus obtained the relation (see for instance [8]) $\alpha+\beta = 3$.

To test this prediction, we compute for different Rh the exponent β from $P(\tau)$ on the time interval $f_t^{-1} < \tau < f_c^{-1}$ corresponding to the frequency interval used to calculate the slope of the spectra. The exponents β are displayed in Fig. 5 together with $\alpha+\beta$. We observe that $\alpha+\beta$ is close to 3. Our experimental measurements are thus in good agreement with the theoretical prediction. We also stress that for $2 < \beta < 3$, the relation $\alpha = 3-\beta$ still holds, even if the PDF of waiting time is asymmetric between *up* and *down* states [8]. This implies that the relation is robust to possible imperfections of the experimental set-up, which could break the symmetry between the two directions of rotation.

Conclusions. – We conclude that the $1/f^{\alpha}$ spectrum is related to the power-law scaling of the PDF of the sojourn time in each polarity of the large scale flow. This observation raises two questions: first, are the $1/f^{\alpha}$ spectra observed in other turbulent flows also related to the statistical properties of coherent structures? Second, what is the origin of the power law distributions of lifetimes of large scale structures in 2D turbulence or other turbulent flows?

Motivated by our observations on 2D turbulence, we considered data for the pressure fluctuations in 3D turbulence [13]. We confirmed that the $1/f^{\alpha}$ spectrum of pressure is related to the power-law scaling of the waiting time between successive pressure drops due to intermittent vorticity filaments. We made a similar observation for the $1/f^{\alpha}$ spectrum of the magnetic field generated by a dynamo process [15] that results from the statistics of bursts of magnetic field. We also believe that the $1/f$ spectrum of the velocity in the von Karman flow [14] results from the power-law scaling of the switching dynamics of the shear layer. The analysis of all these data will be reported elsewhere [26]. The second question related to the origin of the long lifetimes of the LSC and the power-law scaling of the sojourn time in each polarity is still open. We have observed that the switching dynamics between LSC of opposite polarities is rather complex and involve several intermediate states with different vorticity distributions. Thus, we can assume that the whole switching process requires the successful completion of several independent transitions, a mechanism that is known to generate power law distributions [27].

REFERENCES

[1] DUTTA P. and HORN P. M., *Rev. Mod. Phys.*, **53** (1981) 497.
[2] BERNAMONT J., *Proc. Physical Soc.*, **49** (1937) 138.
[3] VAN DER ZIEL A., *Physica*, **16** (1950) 359.
[4] MANDELBROT B. B. and VAN NESS I. W., *SIAM Rev.*, **10** (1968) 422.
[5] LOWEN S. B. and TEICH M. C., *IEEE Trans. Info. Theory*, **36** (1990) 1302.
[6] MANNEVILLE P., *J. Physique*, **41** (1980) 1235.
[7] GEISEL T., ZACHERL A. and RADONS G., *Phys. Rev. Lett.*, **59** (1987) 2503.

[8] LOWEN S. B. and TEICH M. C., *Phys. Rev. E*, **47** (1993) 992.
[9] NIEMANN M., KANTZ H. and BARKAI E., *Phys. Rev. Lett.*, **110** (2013) 140603.
[10] RALLS K. S. ET AL, *Phys. Rev. Lett.*, **52** (1984) 228.
[11] KUNO M. ET AL, *J. Chem. Phys.*, **112** (2000) 3117.
[12] PERRY A. E., HENBEST S. and CHONG M. S., *J. Fluid. Mech.*, **165** (1986) 163.
[13] ABRY P. ET AL, *J. Physique II*, **4** (1994) 725.
[14] RAVELET F., CHIFFAUDEL A. and DAVIAUD F., *J. Fluid. Mech.*, **601** (2008) 339.
[15] BOURGOIN M. ET AL, *Phys. Fluids*, **14** (2002) 3046.
[16] MONCHAUX R. ET AL, *Phys. Fluids*, **21** (2009) 035108.
[17] MININNI P. ET AL, *Phys. Rev. E*, **89** (2014) 053005 and references therein.
[18] KRAICHNAN R. H., *Phys. Fluids*, **10** (1967) 1417.
[19] SOMMERIA J., *J. Fluid. Mech.*, **179** (1986) 139.
[20] PARET J. and TABELING P., *Phys. Fluids*, **10** (1998) 3126.
[21] SOMMERIA J. and MOREAU R., *J. Fluid. Mech.*, **118** (1982) 507.
[22] HERAULT J., *PhD thesis: Dynamique des structures cohérentes en turbulence magnétohydrodynamique* (Université Paris-Diderot) 2013.
[23] SHATS M., BYRNE D. and XIA H., *Phys. Rev. Lett.*, **105** (2010) 264501.
[24] CRAMER A. ET AL, *Flow Meas. Instrum.*, **17** (2006) 1.
[25] MISHRA P. ET AL, *Phys. Rev. E*, **91** (2015) 053005.
[26] HERAULT J., PÉTRÉLIS F. and FAUVE S., *J. Stat. Phys.*, **161** (2015) 16
[27] MONTROLL E. W. and SHLESINGER M. F, *Proc. Natl. Acad. Sci. USA*, **79** (1982) 3380.